4th Pacific International Conference on Applications of Lasers and Optics (PICALO), 2010

APPLICATION OF FEMTOSECOND OPTICAL FREQUENCY COMB'S TEMPORAL COHERENCE CHARACTERISTIC TO A DISTANT ESTIMATION

Dong Wei, Satoru Takahashi, Kiyoshi Takamasu, Hirokazu Matsumoto

Department of Precision Engineering, The University of Tokyo
Hongo 7-3-1, Bunkyo, Tokyo, Japan

Abstract

The improved frequency-stability and the very broad frequency-band of femtosecond mode-locked optical frequency comb (FOFC) have led to new applications in several precision metrology application areas such as high-precision optical frequency metrology, spectroscopy, and distance measurements. We have analyzed the temporal coherence function of the FOFC. As a result, it has been understood that the temporal coherence peaks exist during the time which is equal to the repetition interval in the traveling direction of the FOFC. In order to make the best use of the temporal coherence characteristic of an FOFC, we propose an FOFC-based multiplex Michelson interferometer that can use as a distant estimation. The present technique is expected to be useful for high-precision measurement of distances for not only science purposes but also industry requirements.

Introduction

Due to their improved frequency-stability and very broad frequency-band, there is considerable interest in the development of novel optical measurement techniques based on the characteristics of femtosecond optical frequency combs (FOFC). In the initial stage, the pioneering works [1-8] were done by the groups at the National Institute of Advanced Industrial Science and Technology (AIST). For example, in 2000, Minoshima and Matsumoto reported a high resolution long distant measurement method by using the phase shift of the stable intermode beats [3].

In recent years, the FOFC-based length measurement methods have become of great interest because of its fundamental role not only in science purposes but also industry requirements. For scientific space mission projects such as DARWIN and LISA, the FOFC is a good choice for high-precision absolute long-distance measurements. For example, see reference [9]. For industry requirements, because the FOFC is expected as a new standard tool of the unit system of "Length" and "frequency", how to perform displacement metrology which directly linked to a frequency standard is a new challenge. And in 2009, the FOFC was specified for a new specified standard instrument of length in Japan. For example, see reference [10].

Most of the works have been done on FOFC-based applied metrology, but there are few reports on the temporal coherence function (TCF) of an FOFC, which is important for interference phenomenon. We had analyzed the temporal coherence function of the FOFC [11-12]. As a result, it has been understood that the coherence peak exists during the time which is equal to the repetitions interval in the traveling direction of the FOFC. Based on this new understanding, new applications can be proposed fairly readily [13-16]. For example, measurement of the average temperature change over a distance of 3 m was demonstrated [13]. Moreover, we proposed FOFC-based tandem interference, the possibility of the length measurement and the length delivery by the proposed system were also reported [14].

The present work focuses mainly on development of FOFC-based metrology methods which make the best use of the temporal coherence characteristic of an FOFC. Here, we describe an FOFC-based multiplex Michelson interference that can use as length estimation by using undersampled interference fringes.

Fortunately, this new approach to distance estimation, by combining an ordinary Michelson interferometer and an unbalanced optical-path interferometer, has its own advantages. First, as shown below, this technique maintains the simplicity of the equipment. Second, the displacement metrology can be achieved without fringe analysis which typically restricted the measurement speed in an ordinary Michelson interferometer scheme.

For simplicity of explanation, we have neglected the dispersion and absorption of the optical devices over the FOFC's illumination bandwidth.

The outline of this report is as followings: Section 2 gives a review of an FOFC light source, the TCF of the

FOFC and interference fringes' formation between different pairs of pulse train, Section 3 investigates experiments, and lastly Section 4 presents a summary.

Principles

For convenience of explanation, first, a summary description of an FOFC in the time domain and in the frequency domain is described. Second, a mathematical description of the TCF of the FOFC is given. Last, to observe the TCF of the FOFC, the interference fringe pattern formed by a modified Michelson interferometer is considered.

FOFC

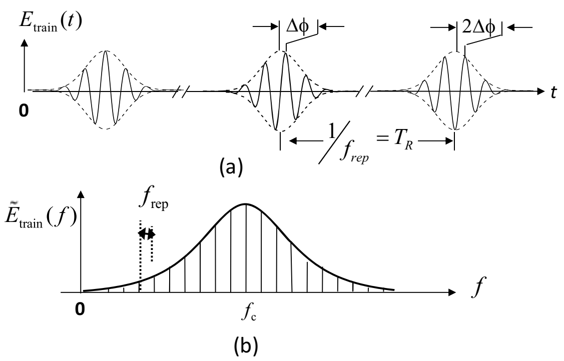

Fig. 1 . Optical comb. (a) Time-domain and (b) frequency domain

The feature of an FOFC can be briefly summarized as following [17]:

① In the time domain, the "carrier" pulse moves with the center carrier frequency f_c of the FOFC. When the electric field packet repeats at the pulse repetition period T_R, the "carrier" phase slips by $\Delta\varphi_{ce}$ to the carrier-envelope phase because of the difference between the group and phase velocities.

② In the frequency domain, a mode-locked FOFC generates equidistant frequency comb lines with the pulse repetition frequency $f_{rep} \propto 1/T_R$, and due to phase slip $\Delta\varphi_{ce}$, the whole equidistant-frequency comb is shifted by f_{CEO}. An FOFC has a large number of (> one million) stable longitudinal modes. Each individual longitudinal mode has a narrow linewidth and tens of nano-watt power.

TCF of FOFC

For convenience of explanation, we herein briefly review and summarize the most important characteristic of the temporal coherence function of an FOFC, which can be founded in derails in Ref.[11]

The power spectrum of an FOFC light source can be expressed as

$$P(f) \propto A(f - f_c) \times \sum_{m=-\infty}^{+\infty} \delta(f - m f_{rep}) , \qquad (1)$$

where $A(f - f_c)$ is the envelope function of the FOFC power spectrum. Based on the Wiener–Khintchine theorem, the interferometric signal of the autocorrelation function is given by the inverse Fourier transform of the spectrum of the source, and we have

$$\gamma(\tau) \propto \mathrm{F}^{-1}\left[A(f - f_c)\right] \otimes \sum_{m=-\infty}^{+\infty} \delta(\tau - m T_R) , \qquad (2)$$

From Eq. (2), the temporal coherence function periodically displays a high temporal coherence peak where the pulse trains signal of the FOFC displays a high-intensity peak with the pulse repetition period T_R.

Interference fringes' formation

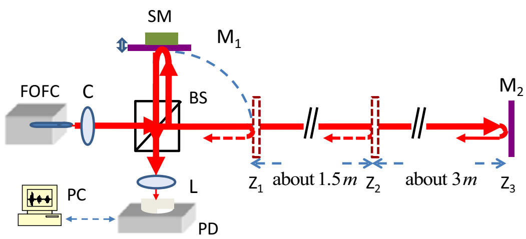

Fig. 2. Optical layout for a modified Michelson interferometer.

Next, let us consider the interference fringe pattern formed by a modified Michelson interferometer shown in Fig. 2. Firstly the incoming pulse train is split into two identical parts $E_{train1}(t)$ and $E_{train2}(t)$ at the beam splitter BS, relatively $E_{train2}(t)$ delays to $E_{train1}(t)$ and they finally are recombined them at the BS. (see Fig. 3).

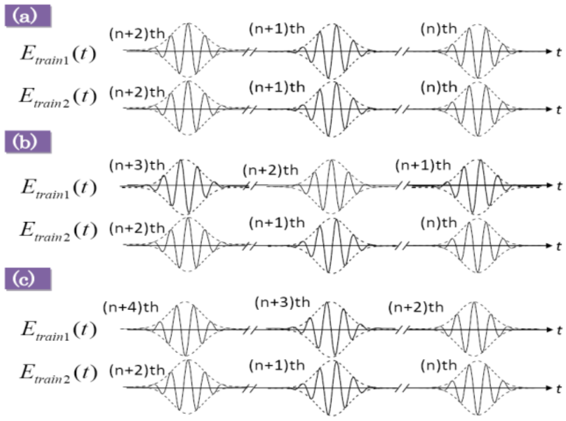

Fig. 3. Relative delays between two pairs of pulse trains. (a) Relative positions at Z_1. (b) Relative positions at Z_2. (c) Relative positions at Z_3.

When the pulse trains overlap in space, one would expect that interference fringes can be observed, as shown in Fig. 1(b). After performing the time integration we obtain

$$I(\tau) \propto |\gamma(\tau)| \cos[\mathrm{mod}(h \times \Delta\varphi_{ce}, 2\pi)]. \qquad (3)$$

Experiment

For convenience of explanation, first, the generation of the interference fringes formed between different pulse trains is confirmed with the modified Michelson interferometer as introduced by the principle. Second, a description of a multiple Michelson interferometer is given. Last, applying the FOFC-based multiplex Michelson interference, a technique that can use as length estimation by undersampled interference fringes is described.

Interference fringes formed with different pulse trains

The basic scheme of the first experiments is considered which is as same as the setup as shown in Fig. 2. The experiment is carried out with a system consisting of an FOFC (FC1500, Menlo Systems, $f_{rep} = 100\,\mathrm{MHz}$), the modified Michelson interferometer, and system controls. The pulse trains from the FOFC is expanded and collimated by a collimator C_1 and introduced into the modified Michelson interferometer. The modified Michelson interferometer are composed of a beam splitter BS, a reference mirror M_1, and an object mirror M_2. During the measurement, by moving the reference mirror M_1 of the interferometer by means of a computer-controlled ultrasonic stepping motor SM, we observed the interference fringes. To obtain the interference fringes formed between different pulse trains, the object mirror is placed by the relative optical displacement Z_2 (about 1.5 m) and Z_3 (about 3 m) from the position Z_1, respectively. After travelling different path lengths, these two pairs of pulse trains overlap at the BS. Lens L_1 images the interference fringes onto a photo detector PD.

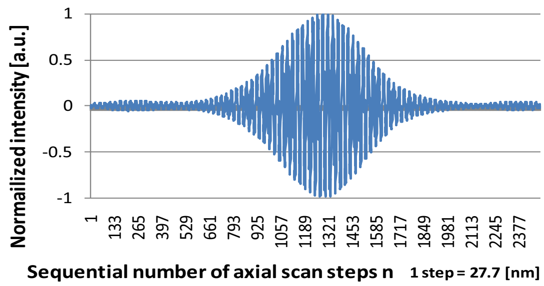

Fig. 4. Interference fringes formed with two pairs of different pulse trains when object mirror M_2 is placed at relative positions Z_1.

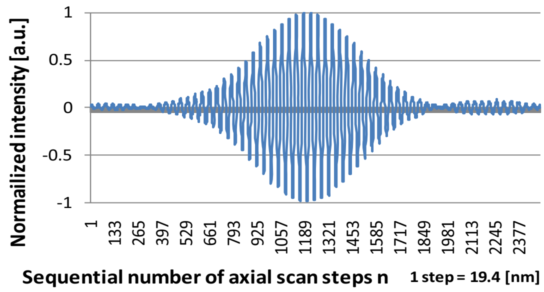

Fig. 5. Interference fringes formed with two pairs of different pulse trains when object mirror M_2 is placed at relative positions Z_2.

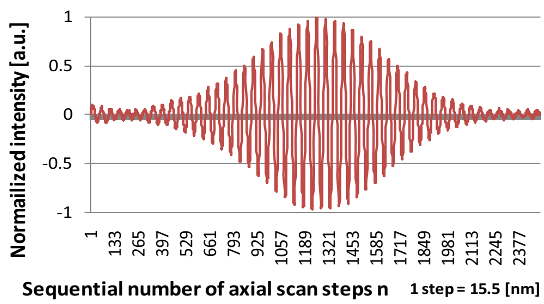

Fig. 6. Interference fringes formed with two pairs of different pulse trains when object mirror M_2 is placed at relative positions Z_3.

Figures 4-6 illustrate the acquired interference fringes with the different relative optical displacement.

Interference fringes formed by a multiple Michelson interferometer

The basic scheme of the second experiments is shown in Fig. 7. The modified Michelson interferometer is a combination of an ordinary Michelson interferometer and two unbalanced optical-path Michelson interferometer. The ordinary Michelson interferometer is composed of a beam splitter BS, a reference mirror M_1, and an object mirror HM_1. The unbalanced Michelson interferometer is composed of the same BS and M_1, and a different object mirror set BS_2 and M_2 to vary the relative delay between the three pulse trains, which are reflected by half-reflecting mirror HM_1, BS_2 and mirror M_2, respectively. During the measurement, by moving the common reference mirror M_1 of the three interferometers by means of a computer-controlled ultrasonic stepping motor SM, we could observe the interference fringes. After travelling different path lengths, these three pairs of pulse trains overlap at the BS.

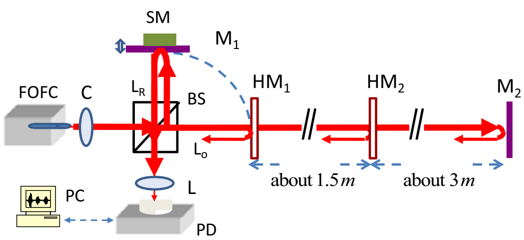

Fig. 7. optical layout for a multiple Michelson interferometer. Abbreviations are defined in the text.

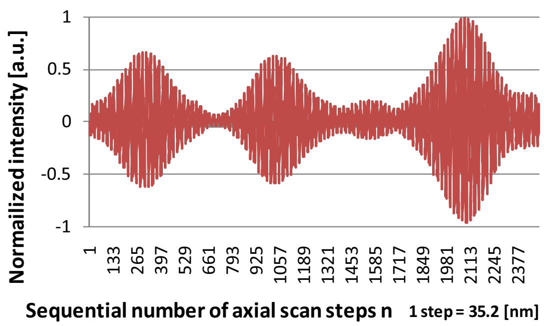

Fig. 8. Interference fringes formed by a multiple Michelson interferometer

In Fig. 8 we show the acquired interference fringes recorded when after travelling different path lengths, these three pairs of pulse trains sequentially overlapped at the beam splitter. The interference fringe signals also exhibit high contrasts between the three pairs of pulse trains by the relative displacements about 0.0 m, 1.5 m and about 3.0 m.

Undersampled interference fringes formed by an ordinary Michelson interferometer

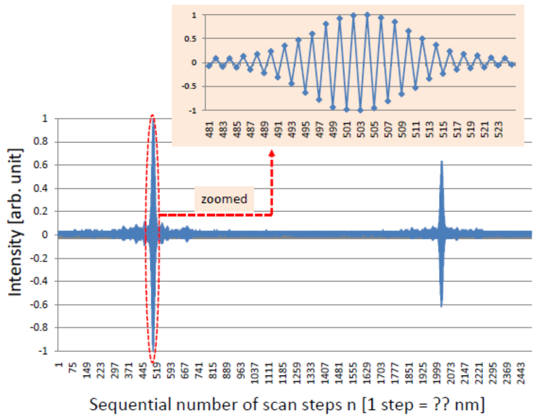

Fig. 9. Undersampled interference fringes formed by an ordinary Michelson interferometer

Figure 9 illustrates the acquired interference fringes with the relatively large optical displacement (> 1 mm). Due to the restricted resolution of the oscilloscope, the undersampled interference fringes are recorded. Because the sampling theorem did not satisfy as noted in Fig.9, the Fourier transform method was not able to be applied for fringe processing. However, to obtain the relative average depth difference we need to get length information from the fringes pattern as shown in Fig.9.

Undersampled interference fringes formed by a multiple Michelson interferometer and distance estimation

Figure 10 illustrates the acquired interference fringes formed by a multiple Michelson interferometer. (For simplicity of explanation, the half-reflecting mirror HM_2 is removed from the second experimental system.)

Figure 10 shows the result when a 500-µm step displacement by the shift of M_2 was repeatedly induced over a distance range of 1000 µm. As noted in Fig. 4, the second interference fringes peak moves away from the first interference fringes peak when the object mirror is moved. We fitted the centers of the peaks, and measured the relative scan steps between the two peaks. The obtained scan step value of the change in relative displacement is 2.0±0.1 µm.

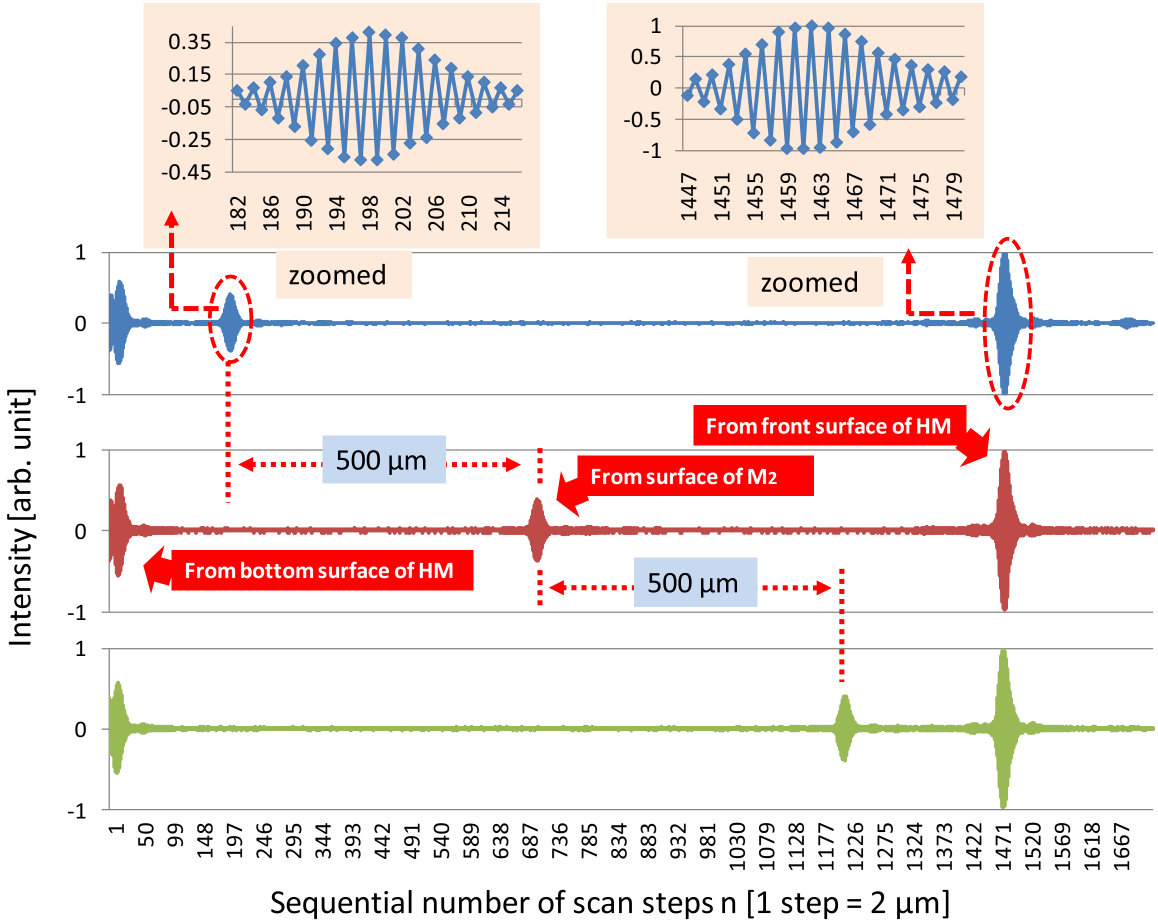

Fig. 8. Distance estimation based on undersampled interference fringes formed by a multiple Michelson interferometer.

And as show in Table 1, we obtained the good linearity between the change in the step displacement shift of M_2 and the relative scan steps.

The relative average depth difference of two surfaces was measured as 2.9 ± 0.1 mm. According to the catalog, the theoretical value of the relative displacement is 3.0 ± 0.1 mm. The measured result of distance is in good agreement with the set distance value within a standard deviation.

Table 1 Relationship between the step displacement shift of M_2 and relative scan steps

Shift of M_2 [µm]	50	100	100	400	500	500
Shift of Peak [steps]	48	108	95	395	504	500

Summary

In summary, we have presented a novel interferometry technique using an FOFC to measure the depth difference by undersampled interference fringes with a multiple Michelson interferometer. The unique feature of an FOFC-based multiple Michelson interferometer is that high temporal coherence peaks can be observed between different pairs of pulse trains from the FOFC light source. And the length information can be recorded and calibrated by interference fringes between different pairs of pulse trains which are located in separated places. The proof-of-the-principle experiments were presented and validated the proposed technique. The present technique is expected to be useful for not only surface profilometry but also tomography.

Acknowledgments

This research work was partially financially supported by the "Development of System and Technology for

Advanced Measurement and Analysis" program at the Japan Science and Technology Agency (JST) and the Global Center of Excellence (GCOE) Program on "Global Center of Excellence for Mechanical Systems Innovation (GMSI)" granted to The University of Tokyo, from the Japanese Government. D. Wei gratefully acknowledges the scholarship given by Takayama International Education Foundation, Heiwa Nakajima Foundation, and Ministry of Education, Culture, Sports, Science, and Technology of Japan (MEXT), respectively.

References

[1] K. Minoshima, H. Matsumoto, Z. Zhang, and T. Yagi (1994) Simultaneous 3-D Imaging Using Chirped Ultrashort Optical Pulses, Japanese journal of applied physics. Letters **33**, L1348-L1351.

[2] K. Minoshima and H. Matsumoto (1997) In-situ measurements of shapes and thicknesses of optical parts by femtosecond two-colour interferometry, Optics Communications **138**, 6-10.

[3] K. Minoshima and H. Matsumoto (2000) High-Accuracy Measurement of 240-m Distance in an Optical Tunnel by Use of a Compact Femtosecond Laser, Appl. Opt. **39**, 5512-5517.

[4] T. Yasui, K. Minoshima, and H. Matsumoto (2000) Three-Dimensional Shape Measurement of a Diffusing Surface by Use of a Femtosecond Amplifying Optical Kerr Gate, Appl. Opt. **39**, 65-71.

[5] T. Yasui, K. Minoshima, and H. Matsumoto (2000) Three-Dimensional Shape Measurement of a Diffusing Surface by Use of a Femtosecond Amplifying Optical Kerr Gate, Appl. Opt. **39**, 65-71.

[6] Y. Yamaoka, K. Minoshima, and H. Matsumoto (2002) Direct Measurement of the Group Refractive Index of Air with Interferometry between Adjacent Femtosecond Pulses, Appl. Opt. **41**, 4318-4324.

[7] Yoshihisa, M. Kaoru, M. Hirokazu, and Z. Lijiang (2003) Deformations of femtosecond pulses after hundred-meter propagation in air with sharp water vapor absorption lines, in Conference on Lasers and Electro-Optics/Quantum Electronics and Laser Science Conference, Technical Digest (Optical Society of America, San Francisco ,USA, CThM1.

[8] Y. Yamaoka, L. Zeng, K. Minoshima, and H. Matsumoto (2004) Measurements and Numerical Analysis for Femtosecond Pulse Deformations After Propagation of Hundreds of Meters in Air with Water-Vapor Absorption Lines, Appl. Opt. **43**, 5523-5530.

[9] I. Coddington, W. C. Swann, L. Nenadovic, and N. R. Newbury (2009) Rapid and precise absolute distance measurements at long range, Nat Photon **3**, 351-356.

[10] I. Hajime, O. Atsushi, N. Yoshiaki, and H. Feng-Lei (2009) optical frequency comb and specified standard instrument of length, Measurement standards and metrology management **59**, 2-8.[in Japanese]

[11] D. Wei, S. Takahashi, K. Takamasu, and H. Matsumoto (2009) Analysis of the temporal coherence function of a femtosecond optical frequency comb," Opt. Express **17**, 7011-7018.

[12] D. Wei, S. Takahashi, K. Takamasu, and H. Matsumoto (2009) Study on the temporal coherence function of a femtosecond optical frequency comb, in *Optical Measurement Systems for Industrial Inspection VI*, Munich, Germany, 73891-73898.

[13] D. Wei, S. Takahashi, K. Takamasu, and H. Matsumoto (2009) Simultaneous Observation of High Temporal Coherence between Two Pairs of Pulse Trains Using a Femtosecond-Optical-Frequency-Comb-Based Interferometer, Japanese journal of applied physics **48**, 070211.

[14] D. Wei, S. Takahashi, K. Takamasu, and H. Matsumoto (2009) Femtosecond optical frequency comb-based tandem interferometer, Journal of the European Optical Society - Rapid publications **4**, 09043.

[15] D. Wei, S. Takahashi, K. Takamasu, and H. Matsumoto (2009) Experimental observation of pulse trains' destructive interference with a femtosecond optical frequency-comb-based interferometer, Opt. Lett. **34**, 2775-2777.

[16] D. Wei, S. Takahashi, K. Takamasu, and H. Matsumoto (2009) Advanced optical metrology of geometrical quantity based on pulse trains' destructive interference geometrical quantity based on pulse trains' destructive interference, in 3rd International Conference of Asian Society for Precision Engineering and Nanotechnology (ASPEN), Kitakyushu, Japan, 1D13.

[17] J. Ye and S. T. Cundiff (2005) Femtosecond optical frequency comb : principle, operation, and applications, Springer, 361 p.